Integral Equation Study of the Surface Tension of Colloidal−Fluid Spherical Interfaces

Fernando Bresme*

Department of Chemistry, Imperial College of Science, Technology and Medicine, Exhibition Road, London, SW7 2AY, United Kingdom

Received: February 28, 2002; In Final Form: May 30, 2002

The surface tension of colloid−fluid spherical interfaces is calculated in the context of the Ornstein−Zernike integral equation. We study models consisting of one colloidal particle immersed in a vapor phase and in low-density fluids at supercritical conditions. This paper focuses on the calculation of the surface tension of the substrate−fluid interfaces via integral equations. We consider a methodology based on the calculation of the chemical potential of the colloid in the fluid. This idea constitutes the basis of the celebrated *scaled-particle theory*. Analysis of a wide range of colloidal sizes and colloid−fluid interaction strengths shows that traditional theories, such as the hypernetted chain integral equation, accurately predict the surface tension of colloid−vapor spherical interfaces of a few nanometers size. We also consider theoretical approaches which incorporate the bridge function, such as the Percus−Yevick theory. The accuracy of these theories to describe the structure of the adsorbed fluid and surface tensions of colloids immersed in fluids at different conditions is discussed.

I. Introduction

The calculation of interfacial surface tensions is relevant to study wetting problems of considerable practical relevance. Recent methodologies on synthesis of nanoparticle monolayers, such as TiO_2 monolayers, are based on the trapping of nanoparticles at the water−air interface.[1] This is essentially a wetting problem as it depends on the balance of the surface tensions of the interfaces formed between the colloid and the different bulk phases.[2] Wetting phenomena of small substrates is also relevant in separation processes, for instance, in gold recovery using solvents in supercritial conditions.[3] In addition, the adsorption of fluids on small spherical substrates is a subject of current interest in the chemical engineering community because it is relevant to the stability of mixtures at supercritical conditions.[4−7] On the fundamental side, adsorption phenomena on curved surfaces are important in colloidal chemistry, in particular in the study of colloidal depletion forces.[8−11]

Wetting of curved surfaces presents several fundamental differences with respect to the wetting of planar surfaces. Curvature inhibits the first-order wetting transition observed in the planar case. A practical consequence of this is that the wetting layer cannot reach an infinite thickness.[12−15] On the other hand, the wetting temperature changes with curvature, increasing as the size of the substrate diminishes. Theoretical studies suggest that deviations from the planar geometry, for instance due to the roughness of the substrate, result in enhanced wetting,[16−18] an effect that has also been observed in experiments.[19] The interesting phenomenology associated to curved interfaces has motivated a number of theoretical works and a significant understanding on wetting of spherical and curved substrates has been achieved in recent years.[20−24] Adsorption on spherical surfaces has also been the subject of computer simulations studies.[10,23,25,27] Recently, we considered the wetting of colloidal particles at liquid−vapor interfaces.[26−28] The wetting behavior was analyzed in terms of the surface tensions and line tensions of the different interfaces. We found that macroscopic expressions, such as Young's equation and Neumann's triangle construction,[29] are surprisingly accurate describing the wetting of nanoscale interfaces, such as those appearing in colloids and nanolenses at fluid−fluid interfaces.[30] The analysis of wetting in these systems via Young's equation relies in the accurate estimation of the surface tension of the colloid−fluid interface. To calculate the surface tensions we introduced a methodology based on the calculation of the free energy change associated to changes in the surface area of the interface. This route does not require the calculation of the pressure tensor[31−33] and constitutes the basis of the *scaled particle theory*, introduced by Reiss, Frisch, and Lebowitz in the late fifties.[34] An approach similar to ours has been used by different authors to study surface tensions of cavities in liquids.[35] We point out that knowledge of the surface tensions can be used to analyze the wetting behavior of three phase systems involving nanometer scale interfaces (see, for instance, ref 27). Also, knowledge of the surface tension of colloidal systems is important to study colloid separation processes or aggregation phenomena in supercritical conditions.

In this paper we study a model consisting of one colloidal particle immersed in a vapor and low-density supercritical phases. We have considered different states for the vapor, and in this way we make connection with previous simulation work.[26,27] The main aim of this paper is to introduce a methodology to calculate surface tensions of spherical interfaces employing integral equations theories, and analyze the accuracy of these theories to study the structure of the fluid adsorbed on the spherical substrate. We have considered three theoretical approximations: hypernetted chain equation (HNC), Percus Yevick (PY), and one approximation to the bridge function proposed by Duh and Henderson (DH).[40] The latter theory has been taken here as representative of a number of new ap-

* To whom correspondence should be addressed. E-mail: f.bresme@ic.ac.uk.

10.1021/jp0205721 CCC: $22.00
Published on Web 07/18/2002

proximations to the bridge function based on the partition of the pair potential following a perturbative scheme. We have solved these theories for a wide range of colloidal sizes and colloid−fluid interaction strengths. Our results show that the surface tensions of the colloids immersed in low density fluids can be accurately obtained using integral equation theories. These theories can also predict reasonably well the surface tensions of colloids immersed in moderate density fluids.

II. Ornstein−Zernike Integral Equation Theories and the Calculation of the Surface Tension

Let us consider one colloidal particle, or in general one spherical substrate, in a fluid. The surface tension of the substrate−fluid spherical interface can be defined through,[26,34,36]

$$dA = 8\pi R_s \gamma \, dR_s + 4\pi R_s^2 P_{out} \, dR_s \quad (2.1)$$

where dA represents the change in the free energy due to an isothermal and reversible increase/decrease of the colloid radius. We note that this increase/decrease in the radius involves a differential change of the interface area, which is proportional to the *surface tension* (γ), and also a differential change in volume, given by the second term in eq 2.1. P_{out} is the bulk fluid pressure, and is taken as the pressure of the fluid far from the surface. Finally, R_s is the surface of tension of the interface.[29]

The calculation of the surface tension via eq 2.1 requires the estimation of the free energy. In this paper we will use the Ornstein−Zernike (OZ) integral equation, but the method is general and can be used in conjunction with any other theoretical approach or computer simulations.

The Ornstein−Zernike integral equation for the general case of a mixture is given by

$$h_{ij}(r_{12}) - c_{ij}(r_{12}) = \sum_k \rho_k \int c_{ik}(r_{13}) h_{kj}(r_{32}) \, d\mathbf{r}_3 \quad (2.2)$$

where h represents the total correlation function, c the direct correlation function, and ρ_k the density of particles of type k. In addition we consider the closure relation

$$h_{ij}(r) = \exp(-\beta u_{ij}(r) + s_{ij}(r) + B_{ij}(r)) - 1 \quad (2.3)$$

where $\beta = 1/k_B T$, k_B is the Boltzmann constant, T is the temperature, $s_{ij} = h_{ij} - c_{ij}$ is the indirect correlation function, and B is the bridge function. The chemical potential of the colloid in the fluid, μ, is related with the free energy through

$$\frac{\beta(A - A^{id})}{N} = 1 + \frac{\beta}{\rho} \sum_i \rho_i (\mu_i - \mu_i^{id}) - \frac{\beta P}{\rho} \quad (2.4)$$

Now let us consider a reversible increase/decrease of the radius of the colloid. Provided the pressure and bulk fluid chemical potential are constant, the change in free energy is given by

$$\frac{dA}{dR_s} = \frac{d\mu_{colloid}}{dR_s} \quad (2.5)$$

which represents a direct relation between the chemical potential of the colloid in the fluid and the free energy change. The chemical potential of the colloid can be obtained through the pair correlation functions and the bridge functions[37,38,40]

$$\beta\mu_i^{res} = 4\pi \sum_j \rho_j \int_0^\infty r^2 \left(\frac{h_{ij}^2(r)}{2} - c_{ij}(r) - \frac{1}{2} h_{ij}(r) c_{ij}(r) + B_{ij}(r) g_{ij}(r) - h_{ij}(r) \int_0^1 B_{ij}(r;\chi) \, d\chi \right) dr \quad (2.6)$$

where $\beta\mu_i^{res}$ is the residual chemical potential, $\beta\mu^{res} = \beta(\mu_i - \mu_i^{id})$. The chemical potential along with eqs 2.1 and 2.5 provides the route to calculate the surface tension of the spherical interface. There is one final element to complete the theory. We need to define the value of the surface of tension, R_s. A good approximation is to take R_s equal to the radius of the colloidal particle, R. We have shown in computer simulation studies,[27] that this choice provides surface tensions which are consistent, when extrapolated to the planar limit, with the surface tension of the corresponding wall−fluid system.

Now it only remains to calculate the chemical potentials. We have considered three integral equation theories: hypernetted chain equation (HNC), Percus−Yevick (PY), and a bridge functional proposed by Duh and Henderson (DH).[40] The expression for the chemical potential in the HNC theory is given by eq 2.6, taking $B_{ij} = 0$. The Percus Yevick chemical potential can be calculated through[39]

$$\beta\mu_i^{res} = \beta\mu_i^{res}(\mathrm{HNC}) + 4\pi \sum_j \rho_j \int_0^\infty r^2 \left(B_{ij}(r) + \frac{h_{ij}(r)}{s_{ij}(r)} \left[s_{ij}(r) - \log(1 + s_{ij}(r)) - \frac{s_{ij}^2(r)}{2} \right] \right) dr \quad (2.7)$$

where $\beta\mu_i^{res}(HNC)$ is the HNC chemical potential, and $B(r)$ is the PY bridge function

$$B_{ij}(r) = \ln(1 + s_{ij}(r)) - s_{ij}(r) \quad (2.8)$$

We note that the expression given above for the chemical potential is not unique. Kjellander and Sarman[39] showed that in the case of approximate theories, such as the PY and related ones, the expression for the chemical potential obtained from the coupling parameter integration method depends on the integration path and consequently it is not unique. These authors also noted that the inaccuracy of the expression 2.7 at high densities was related with the degree of inconsistency of the approximation. Nevertheless the same authors showed for the case of hard spheres that this approximation is very accurate in the low-density regime, a fact already pointed out by Lee.[41] As we are mainly concerned in this paper with surface tensions of substrates in low-density fluids, eq 2.7 represents a good starting point to calculate chemical potentials. We will discuss its accuracy later on. Also we would like to point out that the path dependence problem does not affect the HNC theory, where the chemical potential can be exactly calculated in terms of the pair correlation functions (see eq 2.6 and ref 39).

The DH approximation incorporates a bridge functional which is also a function of $s(r)$, but in addition, the pair potential is partitioned into "reference" and "perturbation" parts, in the spirit

of the WCA theory.[42] The DH bridge function has the following form:

$$B(s(r)) = \begin{cases} \dfrac{-p^2(r)}{2}\left(1+\left(\dfrac{5p(r)+11}{7p(r)+9}\right)p(r)\right) & \text{for } p \geq 0 \\ -\dfrac{1}{2}p^2(r) & \text{for } p < 0 \end{cases} \quad (2.9)$$

where p is given by

$$p(r) = s(r) - \beta u_2(r) \quad (2.10)$$

being u_2 the "perturbation" part of the pair potential. The functional forms of the "perturbation" and "reference" parts depend on the pair potential. Duh and Henderson considered a Lennard-Jones model to test their theory, whereas in this work we use a Lennard-Jones/spline (LJ/s) potential.[43] The LJ/s model is closely related to the Lennard-Jones model, but it has a finite range. The functional form we use in this work is the following:

$$U_{ij}(r,s) = \begin{cases} 4\epsilon_{ij}\left[\left(\dfrac{\sigma_f}{r-d}\right)^{12} - \left(\dfrac{\sigma_f}{r-d}\right)^{6}\right] & \text{if } 0 < r-d < r_{s,ij} \\ a_{ij}(r-d-r_{c,ij})^2 + b_{ij}(r-d-r_{c,ij})^3 & \text{if } r_{s,ij} < r-d < r_{c,ij} \\ 0 & \text{if } r_{c,ij} < r-d \end{cases} \quad (2.11)$$

where r is the distance between particles, σ_f is the diameter of the solvent particles, ϵ_{ij} is the potential depth for interactions i and j, and $d = (\sigma_c - \sigma_f)/2$, being σ_c the diameter of the colloidal particle. The other constants in eq 2.11 are given by $r_{s,ij} = (26/7)^{1/6}\sigma_f$, $r_{c,ij} = (67/48)r_{s,ij}$, $a_{ij} = -(24192/3211)(\epsilon_{ij}/r_{s,ij}^2)$, and $b_{ij} = -(387072/61009)(\epsilon_{ij}/r_{s,ij}^3)$. We note that our model is defined such that the range and strength of the colloid−fluid interactions are independent of the colloid radius even for an infinite radius, where the particle represents a planar wall.

Given the close similarity between the LJ and the LJ/s model, we have chosen Duh and Henderson's functional form to approximate our "perturbation" potential,

$$u_{2,ij}(r) = -4\epsilon_{ij}\left(\frac{\sigma_{ij}}{r-d}\right)^6 \exp\left[\frac{-1}{\rho^*}\left(\frac{\sigma_{ij}}{r-d}\right)^{6\rho}\rho^*\right] \quad (2.12)$$

but taking into account the independence of the range of the potential with the colloid size. The chemical potential for DH bridge functional can be calculated from[40]

$$\beta\mu_j^{res} = \beta\mu_j^{res}(HNC) + 4\pi\sum_j \rho_j \int_0^\infty r^2\left(B_{ij}(r)g_{ij}(r) - \frac{h_{ij}(r)}{p_{ij}(r)}\int_0^{s_{ij}} B_{ij}(s')ds'\right)dr \quad (2.13)$$

with

$$\int_0^s B(s')ds' = \begin{cases} \dfrac{81}{50}s - \dfrac{7}{20}s^2 - \dfrac{9}{2}\ln\left(1+\dfrac{s}{3}\right) - \dfrac{9}{125}\ln\left(1+\dfrac{5s}{3}\right) & \text{for } s \geq 0 \\ -\dfrac{1}{6}s^3 & \text{for } s < 0 \end{cases} \quad (2.14)$$

Finally, regarding the numerical solution of the integral equations, we have employed a Newton−Raphson procedure(see ref 44), with a grid of 4086 points and a mesh of $\delta r = 0.01\sigma_f$.

TABLE 1: Thermodynamic Properties of the LJ/s Potential, Corresponding to $T^* = 0.75$[a]

	$\rho^* = 0.045$			$\rho^* = 0.675$		
	U^*	P^*	$\beta\mu$	U^*	P^*	$\beta\mu$
HNC	−0.422	0.0255	−3.592	−3.475	0.624	−2.120
PY	−0.416	0.0255	−3.592	−3.441	0.874	−3.706
DH	−0.416	0.0255	−3.592	−3.522	0.138	−3.149
MD	−0.410(2)	0.0256(7)	−3.587(3)	−3.565(3)	0.025(1)	−3.56(2)

[a] Values in parentheses represent the error associated to the data.

III. Results

A. Fluid Structure around the Colloidal Particle. In the following we discuss the adsorption of the fluid on the spherical substrate. We have considered one colloid of variable size immersed in vapor and supercritical states. The densities of the vapor phases correspond to the vapor coexistence densities of the Lennard-Jones spline model, obtained from molecular dynamics computer simulations of the liquid−vapor interface. In previous work we studied in detail via molecular dynamics one of these states, corresponding to $T^* = 0.75$; therefore, it constitutes an excellent reference to test the theoretical approximations considered in this paper. Table 1 compiles simulation and integral equation results for the pressure, internal energy and chemical potentials. The computer simulation data were obtained via molecular dynamics simulations in the canonical ensemble. Details on the computer simulations can be found in our previous work.[27] The HNC integral equation is very accurate describing the properties of the vapor phase but rather inaccurate in the case of the liquid. Incorporation of the bridge functions solves in part this problem. Indeed, the PY theory is particularly successful predicting the chemical potential, but unfortunately the pressure is largely overestimated. In this sense the DH theory as implemented in this work, provides a more accurate description of the liquid state. This is consistent with the good results obtained by Duh and Henderson in their study of the coexistence curve of the Lennard-Jones potential. We will see later that current theories can be rather inaccurate describing high density states, but rather accurate for intermediate densities. The aim of this paper is to illustrate the calculation of surface tensions via integral equations, and for this purpose we will focus in the low/intermediate density region, where current integral equation theories are more accurate.

Figure 1 summarizes our results for colloid−vapor density profiles as a function of colloid size and for two representative vapor−colloid interaction strengths. The density profile of large colloids shows a small decrease in the local density defined by the first adsorption layer. This resembles the changes observed in the local solvent density of supercritical fluids surrounding small particles.[5] The HNC theory accurately predicts these changes, and the agreement with the simulation results for $\epsilon_{cf} = 1.25\epsilon_{ff}$ is particularly remarkable. Increase in the colloid−fluid interaction strength increases the adsorption of the vapor on the colloidal particle (see Figure 1, $\epsilon_{cf} = 1.5\epsilon_{ff}$), and in this case some of the deficiencies of the HNC theory become apparent, in particular in the inability to predict the second layer (cf. Figure 1). It is reasonable that upon an increase in the density some of the correlations disregarded by the HNC equation can become important. These correlations can be contemplated through the bridge functions. Indeed, PY and DH theories show that the introduction of the bridge function leads to an accurate description of the density profiles, particularly

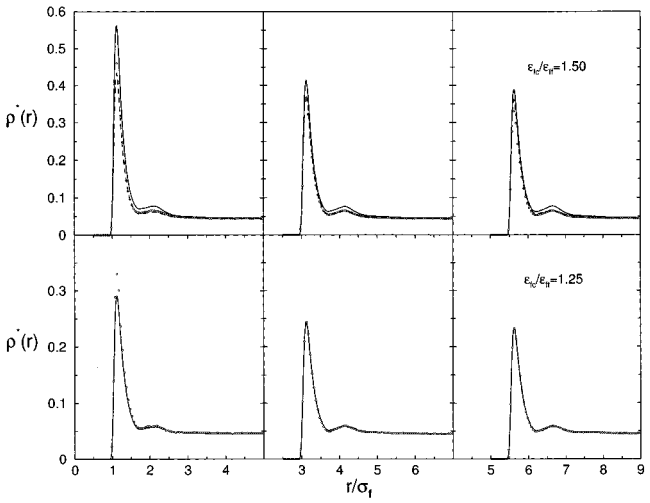

Figure 1. Vapor−colloid density profile as a function of colloid size, 1, 5, and 10 σ_f and interactions strengths 1.25 and 1.50 ϵ_{ff}. The symbols represent molecular dynamics results and lines results from the integral equation theories. Full lines HNC closure, dashed lines for $\epsilon_{cf} = 1.5\epsilon_{ff}$ PY and DH theories for sizes $\sigma_{cf} = 1$ and 5 σ_{ff} and DH theory for size $\sigma_{cf} = 10\ \sigma_{ff}$.

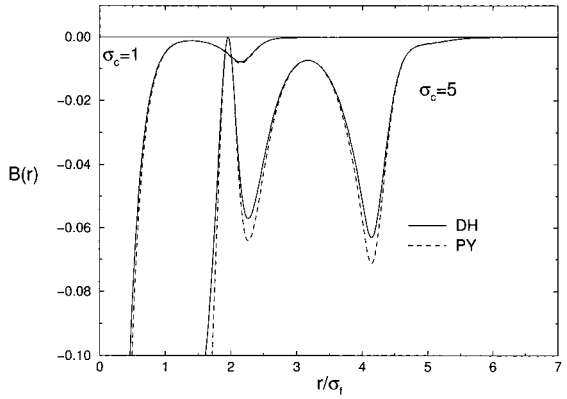

Figure 2. Colloid−vapor bridge functions for colloid sizes 1 and 5 σ_f and $\epsilon_{cf} = 1.5\epsilon_{ff}$.

evident in the second peak of $\rho(r)$. These two theories lead essentially to the same profiles. This similarity is reflected as well in the bridge functions predicted by both approximations (cf. Figure 2).

In addition to the vapor state, we have analyzed the corresponding coexisting liquid at the same temperature, $T^* = 0.75$. Figure 3 shows results for this state as a function of colloid size and for one representative interaction strength, $\epsilon_{cf} = 1.25\epsilon_{ff}$. The HNC and DH theories qualitatively reproduce the structure of the adsorbed liquid, although they tend to underestimate the thickness of the first liquid layer, particularly evident in the largest colloid size considered here ($10\sigma_f$). Clearly this feature is not corrected through the introduction of the bridge functions.

In the following we discuss our results for the colloidal particle immersed in supercritical fluids. Figure 4 show results for a colloid of size $\sigma_C = 10\sigma_f$, and two representative surface-fluid interaction strengths. We have considered two intermediate densities, $\rho^* = 0.1$, $\rho^* = 0.3$, that we will discuss later in the section dealing with the surface tensions results. The supercritical temperature we have chosen is $T^* = 1.0$ slightly higher than the critical temperature of the LJ/s potential, $T^* \approx 0.91$. The HNC theory very accurately describes the density profile of the fluid in different conditions. We find that this theory is more accurate than the PY one (cf. Figure 4). At least in the conditions considered here, the introduction of the bridge function does not lead to an improvement in the description of the structure of the adsorbed fluid.

B. Chemical Potentials. We focus in this section on the calculation of the chemical potentials of the colloids in the vapor and fluid phases. Chemical potentials can provide important information on the stability of dispersions of particles in liquids or depletion forces, but we are concerned here with the calculation of the chemical potential of a colloid, or in general a substrate, to estimate the surface tension of the spherical interface. In the following we compare the chemical potentials predicted by different theories with molecular dynamics simulation results. Again we have chosen $T^* = 0.75$ as a reference to test the different theoretical approximations. The chemical potentials of small particles, $\sigma_c = 1-3\sigma_f$, in the vapor and liquid phases, were obtained using Widom's insertion method,[45] whereas for large colloid sizes we resorted to a perturbation method

$$\beta\mu(\sigma_{col}) = \beta\mu(\sigma_{col} = 1) + \int_1^{\sigma_{col}} \beta\mu'\, d\sigma \qquad (3.1)$$

where $\beta\mu'$ is defined as

$$\beta\mu' = \frac{d(\beta\mu)}{d\sigma} \approx \frac{\Delta(\beta\mu)}{\Delta\sigma} = -\frac{\ln\langle\exp\{-\beta[U(\sigma') - U(\sigma)]\}\rangle_\sigma}{\Delta\sigma} \qquad (3.2)$$

being $U(\sigma')$ and $U(\sigma)$ the potential energies of the "perturbed", $\sigma' = \sigma \pm \Delta\sigma$ and "reference" states, σ. Typical values for $\Delta\sigma$ were $0.01\sigma_f$ for the vapor and $0.005\sigma_f$ for the liquid. All the calculations were done ensuring that the average density of the fluid with respect to the colloid, taken as the mean value at large separations, was equal to the corresponding density of the bulk. We calculated the ensemble average in eq 3.2 for different colloid sizes, going from $\sigma = 1$ to 10 σ_f at intervals of $1\sigma_f$. These values were fitted to a polynomial and the chemical potential was calculated from eq 3.1. These calculations involved around 500000 time steps per colloid. Figure 5 shows the

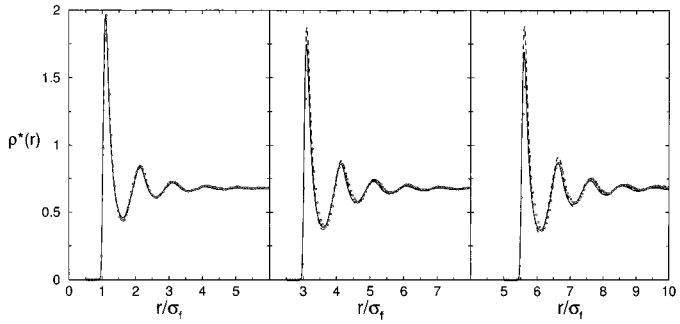

Figure 3. Liquid−colloid density profiles for $\epsilon_{cf} = 1.25\epsilon_{ff}$ and different colloid sizes. Open circles represent molecular dynamics data, full lines HNC integral equation, and dashed lines DH theory.

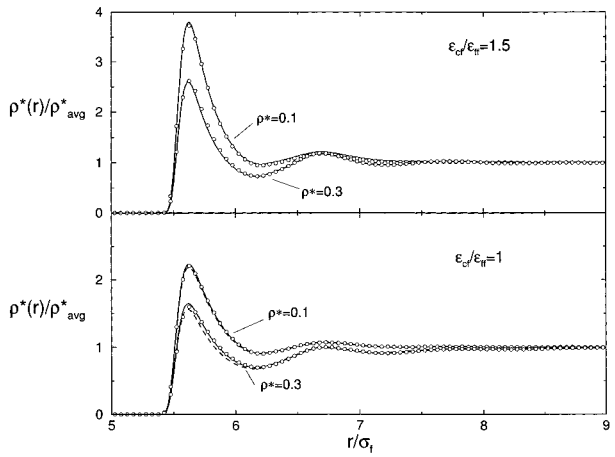

Figure 4. Fluid−colloid density profiles as a function of interaction strength and fluid density. $T^* = 1.0$, $\sigma_c = 10\sigma_f$, and $\epsilon_{cf} = \epsilon_{ff}$. Full lines HNC theory, dot dashed line PY theory, and symbols molecular dynamics simulation data.

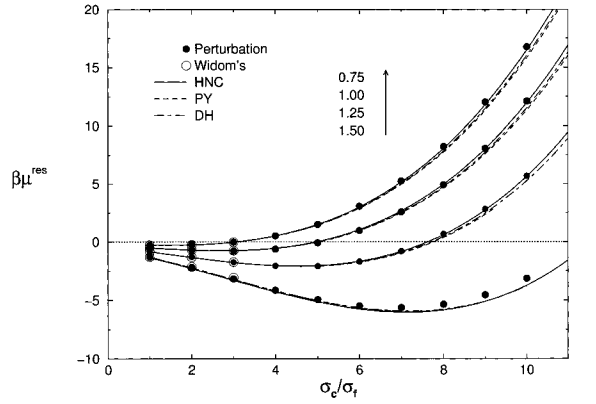

Figure 5. Residual chemical potential of the colloidal particle in the vapor phase as a function of size and interaction strength. Open circles, chemical potential from Widom's insertion method; black circles, perturbation method; full lines, HNC integral equations; dashed lines, PY; and dash−dot DH approximation.

chemical potentials obtained in this way as a function of colloid size and different colloid−fluid interaction strengths, and Table 2 compiles selected data. Our results show that the perturbation and Widom's methods predict chemical potentials which are consistent one each other. We are particularly interested in the performance of the different theories predicting these results. A standard theory, such as the HNC, shows to be very accurate for a wide range of situations. Some small deviations are apparent for the larger interaction strength we have considered ($\epsilon_{cf} = 1.5\epsilon_{ff}$), but as we will see later this does not compromise the accuracy of the theory predicting the surface tensions. Other approximations, PY and DH, do not lead to major improvements in the prediction of the chemical potential, despite the fact they provide a better description of the structure of the vapor surrounding the substrate. Overall the HNC theory approximation seems promising to estimate surface tensions. We will analyze this in detail in the next section.

The theoretical prediction of the chemical potential becomes more problematic when considering colloids immersed in fluids at higher densities. To illustrate this we consider the chemical potential of the colloid in the coexistence liquid phase at $T^* = 0.75$. Approximations, such as DH and PY, accurately predict the chemical potential for small colloidal sizes, $1-2\ \sigma_f$, but they become inaccurate describing colloids of realistic size, $5-10\ \sigma_f$ (see Figure 6). Similar behavior has been reported recently in studies of cavities immersed in Lennard-Jones fluids.[35]

TABLE 2: Excess Chemical Potentials ($\beta\mu$) for Different Size Ratios and Interaction Strengths

		$\rho^* = 0.045$			
$\epsilon_{cv}/\epsilon_{ff}$	σ_c/σ_f	MD	HNC	PY	DH
0.75	1.0	−0.251	−0.251	−0.252	−0.252
	5.0	1.516	1.508	1.456	1.471
	10.0	16.77	16.49	15.82	16.02
1.00	1.0	−0.486	−0.491	−0.490	−0.491
	5.0	−0.063	0.036	−0.009	0.005
	10.0	12.11	11.99	11.33	11.53
1.25	1.0	−0.811	−0.829	−0.829	−0.820
	5.0	−2.08	−2.029	−2.059	−2.047
	10.0	5.70	5.653	-	5.275
1.50	1.0	−1.278	−1.357	−1.305	−1.304
	5.0	−4.93	−5.121	−5.021	−5.015
	10.0	−3.12	−3.716	-	−3.762
		$\rho^* = 0.675$			
$\epsilon_{cl}/\epsilon_{ff}$	σ_c/σ_f	MD	HNC	PY	DH
1.00	1.0	−3.166	−1.727	−3.325	−2.861
	2.0	−1.064	6.879	0.901	3.588
	5.0	14.24	109.6	80.70	110.10
1.25	1.0	−5.683	−4.142	−5.587	−5.270
	2.0	−5.823	2.320	−3.535	−1.183
	5.0	−0.72	94.7		93.3

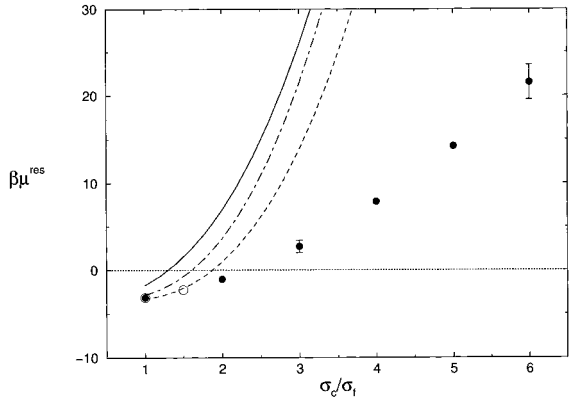

Figure 6. Residual chemical potential of the colloidal particle in the liquid phase for $\epsilon_{cf} = 1\ \epsilon_{ff}$. Symbols have the same meaning as those in Figure 5.

Regarding intermediate densities, i.e., the ones relevant to the supercritical states, one can anticipate that the description will be less accurate the larger the density of the fluid considered. We discuss these cases in the next section where we illustrate this effect with the surface tension results.

C. Surface Tensions. The chemical potentials are the key quantities to access the surface tension of the substrate−fluid interfaces, but looking at eq 2.1, it is clear that the theory has to be accurate also predicting the pressure of the bulk fluid. The HNC theory fulfills these requirements in vapor−colloid interfaces. In Figure 7 we compare the HNC vapor−colloid surface tensions with simulation results taken from reference.[27] The agreement is excellent, showing that the HNC theory along with the method presented in section I, constitutes an excellent approach to calculate surface tensions.

Interestingly the surface tensions predicted by our model are negative for the range of sizes and interactions studied. This resembles the results obtained for hard sphere fluids and hard sphere cavities immersed in Lennard-Jones liquids, where γ is also negative.[21,34] The relative changes in surface tensions for different systems, such as the ones studied here can give

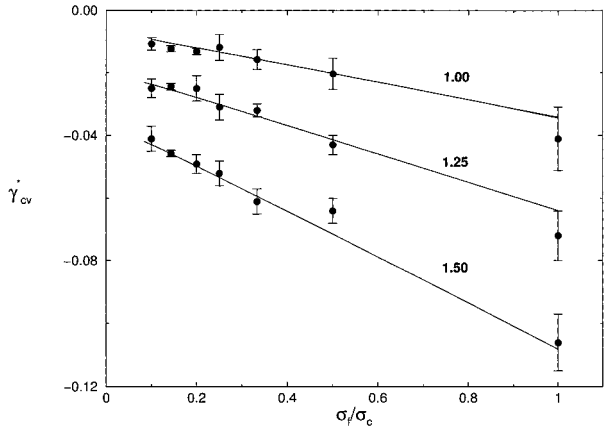

Figure 7. Colloid−vapor surface tensions as a function of the inverse of colloid size and interaction strengths $\epsilon_{cf} = 1$, 1.25, and 1.5 ϵ_{ff}. Points represent simulation data taken from ref 27 and lines HNC integral equation results.

information on the stability of a colloidal dispersion. Thus, positive values for γ would normally indicate the tendency of the colloids to aggregate, as this would minimize the interface surface area, and therefore the free energy. Negative surface tensions could be interpreted in principle as a tendency of the colloids to disperse in the fluid. Nonetheless in order to describe in detail the stability of the dispersion colloid−colloid interactions have also to be taken into account, as these can balance the gain in free energy due to the loss of interfacial area.

Inspection of Figure 7 reveals a clear linear dependence of the surface tensions with the inverse of the colloid diameter. This is similar to the expected dependence of the surface tension observed in liquid droplets for instance. This dependence was addressed by Tolman,[46]

$$\gamma(R) = \gamma_\infty\left(1 - \frac{2\delta}{R}\right) + O(R^{-2}) \qquad (3.3)$$

where γ_∞ represents the surface tension of the planar interface, and $\delta = R_e - R_s$ is the Tolman length, being R_e the position of the equimolar dividing surface in the planar interface, and R_s the surface of tension. Considering Tolman's expression, one expects that the surface tension of the spherical interface will vary, at least at first order, with the inverse of the interface radius. Our results are in agreement with this idea (cf. Figure 7). We find that the values for the Tolman length are rather small, ≈0.025 in colloid−vapor interfaces. This indicates that for these systems, the dependence of γ with curvature is small. Given the nature of the approximation considered to calculate the surface tensions, the values obtained here for the Tolman length should be taken as representative of the order of magnitude expected for these systems, but not as the exact value.

In addition to the state, $T^* = 0.75$ reported above, we have studied the dependence of the colloid−vapor surface tension along the vapor coexistence line of the LJ/s model. These results are reported in Figure 8 for two colloid sizes, $\sigma_c = 5$, 10 σ_f, and two substrate−vapor interaction strengths, $\epsilon_{fc} = \epsilon_{ff}$ and $\epsilon_{fc} = 0.7\epsilon_{ff}$.

Our simulation results show that the surface tension is very sensitive to the substrate fluid interaction. Small changes in substrate−fluid interaction $\epsilon_{fc}/\epsilon_{ff} = 0.7-1$ result in a complete change in the dependence of the surface tension with temperature. For the larger interaction strengths the surface tension becomes more negative with increasing temperature. This would favor the creation of vapor−surface interface and therefore the systems would be stabilized as a dispersion with increasing

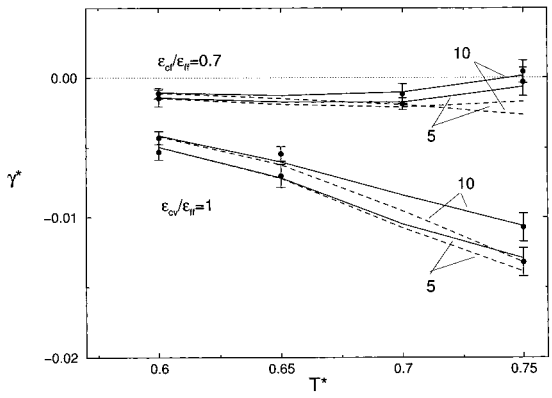

Figure 8. Surface tensions of colloid−vapor interfaces along the vapor branch of the LJ/s model coexistence line: $(T^*,\rho^*) = (0.6,0.0089_{23})$, $(0.65,0.015_1)$, $(0.70,0.028_1)$, $(0.75,0.046_1)$, and $(0.80,0.072_2)$, the subindex represents the error associated to the data. Full lines HNC theory, dashed lines PY theory, and symbols molecular dynamics simulations.

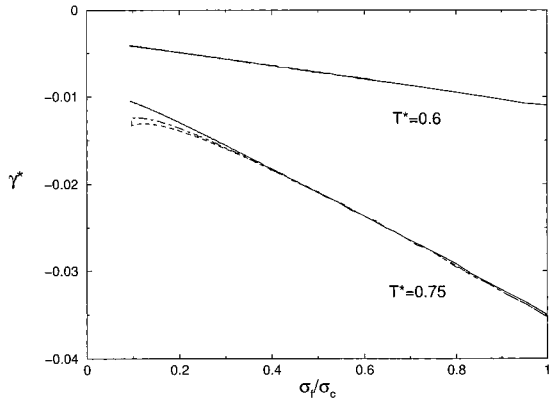

Figure 9. Dependence of the surface tension with colloid size for colloids immersed in vapor phases ($\epsilon_{fc} = \epsilon_{ff}$). Full lines HNC theory, dot−dashed lines PY theory, and dashed lines DH approximation.

temperature. On the other hand, a slight decrease in the interaction strength, $\epsilon_{fc} = 0.7\epsilon_{ff}$, results in a non monotonic behavior in γ^*, and we observe the possible apparition of a minimum in the surface tension as the temperature increases. This features are confirmed by the theoretical calculations. Again the HNC predictions are in excellent agreement with the simulation results confirming the accuracy of this theory.

The nontrivial dependence of the surface tension with temperature and substrate−fluid interaction strength would indicate the possibility of the colloids to pass through different regimes as a function of temperature, going from states where the formation of the interface is slightly favored to others where it is slightly disfavored. Certainly to address the final stability of these systems one would have to take into account also the presence of other colloids and therefore finite colloid concentrations.

In Figure 8 we have also included predictions from the PY theory. We find this theory is less accurate than the HNC for high temperatures, something that contrast with the results we obtained for the density profiles, where we shown the PY theory improves the description of the structure of the vapor surrounding the substrate. In particular it is noticeable the crossing of the surface tensions of colloids of sizes 5 and 10, around $T^* \approx 0.7$, which is incorrect. These results can be explained looking at the dependence of the surface tension with colloidal size predicted by the theories (cf. Figure 9). This shows that PY, DH and HNC approximations predict essentially the same results for low temperatures, ($T^* = 0.6$), but at higher temper-

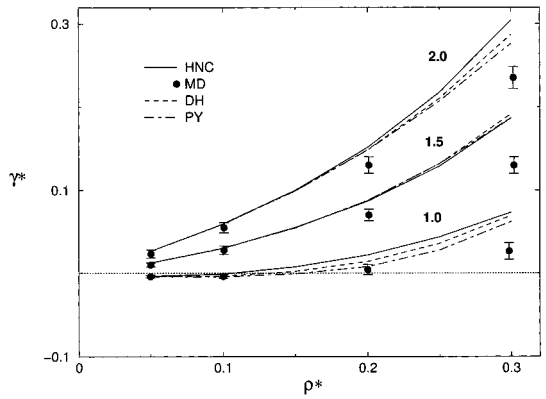

Figure 10. Surface tensions of representative supercritical states as a function of density and temperature. $\sigma_c = 5\sigma_f$ and $\epsilon_{cf} = \epsilon_{ff}$.

atures, ($T^* = 0.75$), PY and DH approximations significantly deviate from the linear behavior observed in the HNC theory. This linear behavior is compatible with the simulation results (see Figure 7) and in this sense the HNC represents a better approximation to calculate surface tensions than the PY and DH ones.

In addition to the vapor states we have analyzed the surface tensions of colloids immersed in supercritical fluids. Figure 10 illustrates the dependence of the surface tension with density, for three supercritical isotherms and for the colloid size $\sigma_c = 5\ \sigma_f$. The theories are rather accurate for intermediate densities, up to $\rho^* = 0.2$, but we observe a trend to consistently overestimate the surface tension as the density increases. One could consider the formation of wetting films to explain the behavior observed at higher densities. It would be interesting to investigate this possibility, but it would require a different approach to the one considered here. In any case the states considered in this work are below the typical interaction strengths necessary to induce wetting of the colloid (see ref 27). We conclude rather that in the cases studied in this work, the inaccuracy of the theories to describe the surface tensions of large colloids immersed in dense phases, is due to their inability predicting accurate chemical potentials (see for instance Figure 6). Despite this all the theories are rather successful predicting the order of magnitude of the surface tension, as well as its dependence with density and temperature.

IV. Summary and Final Remarks

In this work we have presented an integral equation methodology to obtain the surface tension of a colloid−fluid spherical interface. We have illustrated the use of the method with the Ornstein−Zernike equation and also computer simulation results, but in principle it could be employed in different theoretical contexts provided the chemical potentials of substrate−fluid interfaces are accessible.

Integral equation theories such as the HNC and PY account for most of the changes observed in the fluid−colloid adsorption for different colloid sizes and fluid−colloid interactions. Nonetheless, the study of the density profiles, in strong vapor−substrate interaction strength conditions, requires the consideration of theories beyond the HNC. PY and DH theories constitute good approximations in this sense. Regarding dense phases, all the theories considered in this work provide a fair description of typical liquid density profiles around a colloidal substrate. Also the density profiles for supercritical states can be very accurately described using these approximations in particular the HNC closure.

With regard to the main topic of this paper, the calculation of the surface tension, we have shown that the HNC approximation represents an excellent theory to estimate colloid−vapor surface tensions. We have shown it predicts non trivial behavior in the surface tension of subcritical and also supercritical states. The accuracy does not seem to be limited by the substrate−fluid interaction strength neither by temperature. Calculations for supercritical states show that the theories predict the trends and order magnitude of the surface tension at intermediate densities, although increase in the fluid density results in significant deviations. We have shown these are particularly severe for systems involving typical liquid densities. These results emphasize the need for further work to find accurate theories that can cope with the high density regime. Computer simulations could be particularly useful to reach this objective, as they can provide important information on the bridge functionals, a route that has been exploited in the past to study simple fluids. Other alternatives may involve the imposition of thermodynamic self-consistency on the integral equations. Some recent studies on hard sphere systems[47] using the MHNC integral equation have shown that this route can overcome some of the problems observed with approximations such as the Percus−Yevick.

Overall we believe the present methodology might be useful in a number of contexts; colloid separation processes, aggregation in supercritical conditions or wetting of colloids at interfaces.[26,28] In addition integral equation studies of the surface tension of molecular fluids, for instance, through central force models[48,49] or RISM[50] approaches, could also be considered following the ideas presented in this work.

Acknowledgment. The author acknowledges the award of EPSRC Research Grant GR/R39726/01. I am also grateful to Dr. J. A. Anta for helpful comments and discussions.

References and Notes

(1) Fendler, J. H. *Curr. Opin. Colloid Interface Sci.* **1996**, *1*, 202.
(2) Pieranski, P. *Phys. Rev. Lett.* **1980**, *45*, 569.
(3) Shi, C.; Li, J.; Beckman, E. J.; Enick, R. M. *J. Supercrit. Fluids* **2000**, *17*, 81.
(4) Chialvo, A. A.; Debenedetti, P. G. *Ind. Eng. Chem. Res.* **1992**, *31*, 1391.
(5) Tanaka, H. J.; Shen, K.; Nakanishi, K.; Zenk, X. C. *Chem. Phys. Lett.* **1995**, *239*, 168.
(6) Shing, K. S.; Gubbins, K. E.; Lucas, K. *Mol. Phys.* **1988**, *65*, 1235.
(7) Lotfollahi, M. N.; Modarress, H.; Mansoori, G. A. *Can. J. Chem. Eng.* **2000**, *78*, 1157.
(8) Israelachvili, J. *Intermolecular and Surface Forces*; Academic Press: New York, 1998.
(9) Biben, T.; Bladon, P.; Frenkel, D. *J. Phys.: Condens. Matter* **1996**, *8*, 10799.
(10) Dickman, R.; Attard, P.; Simonian, V. *J. Chem. Phys.* **1997**, *107*, 205.
(11) Götzelmann, B.; Evans, R.; Diectrich, S. *Phys. Rev. E* **1998**, *57*, 6785.
(12) Holyst, R.; Poniewierski, A. *Phys. Rev. B* **1987**, *36*, 5628.
(13) Gelfand, M.; Lipowsky, R. *Phys. Rev. B* **1987**, *36*, 8725.
(14) Upton, P. J.; Indekeu, J. O.; Yeomans, J. M. *Phys. Rev. B* **1989**, *40*, 666.
(15) Blohuis, E. M.; Bedeaux, D. *Mol. Phys.* **1993**, *80*, 705.
(16) Parry, A. O.; Swain, P. S.; Fox, J. A. *J. Phys.: Condens. Matter* **1996**, *8*, L659.
(17) Borgs, C.; de Coninck, J.; Koteckýý, R.; Zinque, M. *Phys. Rev. Lett.* **1995**, *74*, 2292.
(18) Netz, R. R.; Andelman, D. *Phys. Rev. E* **1997**, *55*, 687.
(19) Wenzel, R. N. *J. Phys. Colloid Chem.* **1949**, *53*, 1466. Wenzel, R. N. *Ind. Eng. Chem.* **1936**, *28*, 988.
(20) Attard, P. *J. Chem. Phys.* **1989**, *91*, 3083.
(21) Samborski, A.; Stecki, J.; Poniewierski, A. *J. Chem. Phys.* **1993**, *98*, 8958.
(22) Bieker, T.; Dietrich, S. *Phys. A* **1998**, *252*, 85.

(23) Henderson, D.; Sokolowski, S.; Patrykiejew, A. *Mol. Phys.* **1995**, *85*, 745.
(24) Hadjiagapiou, I. *J. Chem. Phys.* **1996**, *105*, 2927.
(25) Stecki, J.; Toxvaerd, S. *J. Chem. Phys.* **1990**, *93*, 7342.
(26) Bresme, F.; Quirke, N. *Phys. Rev. Lett.* **1998**, *80*, 3791.
(27) Bresme, F.; Quirke, N. *J. Chem. Phys.* **1999**, *110*, 3536.
(28) Bresme, F.; Quirke, N. *Phys. Chem. Chem. Phys.* **1999**, *1*, 2149.
(29) Rowlinson, J. S.; Widom, B. *Molecular Theory of Capillarity*; Oxford Science: New York, 1989.
(30) Bresme, F.; Quirke, N. *J. Chem. Phys.* **2000**, *112*, 5985.
(31) Thompson, S. M.; Gubbins, K. E.; Walton, J. P. R. B.; Chantry, R. A. R.; Rowlinson, J. S. *J. Chem. Phys.* **1984**, *81*, 530.
(32) Nijmeijer, M. J. P.; Bruin, C.; van Woerkom, A. B.; Bakker, A. F.; van Leeuwen, J. M. J. *J. Chem. Phys.* **1992**, *96*, 565.
(33) Mareschal, M.; Baus, M.; Lovett, R. *J. Chem. Phys.* **1997**, *106*, 645.
(34) Reiss, J. L.; Frisch, H. L.; Lebowitz, J. L. *J. Chem. Phys.* **1959**, *31*, 369.
(35) Moody, M. P.; Attard, P. *J. Chem. Phys.* **2001**, *115*, 8967.
(36) Henderson, J. R. *Mol. Phys.* **1983**, *50*, 741.
(37) Kirkwood, J. G. *J. Chem. Phys.* **1935**, *3*, 300.
(38) Kiselyov O. E.; Martynov G. A. *J. Chem. Phys.* **1990**, *93*, 1942.
(39) Kjellander, R.; Sarman, S. *J. Chem. Phys.* **1989**, *90*, 2768.
(40) Duh, D. M.; Henderson, D. *J. Chem. Phys.* **1996**, *104*, 6742.
(41) Lee, L. L. *J. Chem. Phys.* **1974**, *60*, 1197.
(42) Weeks, J. D.; Chandler, D.; Andersen, H. C. *J. Chem. Phys.* **1971**, *54*, 5237.
(43) Holian, B. L.; Evans, D. J. *J. Chem. Phys.* **1983**, *78*, 5147.
(44) Lomba, E.; Høye, J. S. *Comput. Phys. Commun.* **1992**, *69*, 420.
(45) Widom, B. *J. Chem. Phys.* **1963**, *39*, 2808.
(46) Tolman, R. C. *J. Chem. Phys.* **1949**, *17*, 333.
(47) Caccamo, C.; Pellicane, G.; Enciso, E. *Phys. Rev. E* **1997**, *56*, 6954.
(48) Bresme, F.; Abascal J. L. F.; Lomba E. *J. Chem. Phys.* **1996**, *105*, 100081996; *J. Chem. Phys.* **1997**, *106*, 1569.
(49) Bresme, F. *J. Chem. Phys.* **1998**, *108*, 4505; *ibid*, **2001**, *115*, 7564.
(50) Chandler, D.; Andersen, H. C. *J. Chem. Phys.* **1972**, *57*, 1930.